Deep-Sea Research I 102 (2015) 16–25

Contents lists available at ScienceDirect

Deep-Sea Research I

journal homepage: www.elsevier.com/locate/dsri

Analytical phytoplankton carbon measurements spanning diverse ecosystems

Jason R. Graff [a,*], Toby K. Westberry [a], Allen J. Milligan [a], Matthew B. Brown [a], Giorgio Dall'Olmo [b], Virginie van Dongen-Vogels [a,1], Kristen M. Reifel [a], Michael J. Behrenfeld [a]

[a] Oregon State University, Department of Botany and Plant Pathology, 2082 Cordley Hall, Corvallis, OR, United States
[b] Plymouth Marine Laboratory, Prospect Place, The Hoe, Plymouth, United Kingdom and National Centre for Earth Observation, United States

ARTICLE INFO

Article history:
Received 24 November 2014
Received in revised form
8 April 2015
Accepted 8 April 2015
Available online 28 April 2015

Keywords:
Phytoplankton carbon
Backscattering
Chlorophyll
Particulate organic carbon
Atlantic Meridional Transect
Satellite

ABSTRACT

The measurement of phytoplankton carbon (C_{phyto}) in the field has been a long-sought but elusive goal in oceanography. Proxy measurements of C_{phyto} have been employed in the past, but are subject to many confounding influences that undermine their accuracy. Here we report the first directly measured C_{phyto} values from the open ocean. The C_{phyto} samples were collected from a diversity of environments, ranging from Pacific and Atlantic oligotrophic gyres to equatorial upwelling systems to temperate spring conditions. When compared to earlier proxies, direct measurements of C_{phyto} exhibit the strongest relationship with particulate backscattering coefficients (b_{bp}) (R^2=0.69). Chlorophyll concentration and total particulate organic carbon (POC) concentration accounted for ~20% less variability in C_{phyto} than b_{bp}. Ratios of C_{phyto} to Chl a span an order of magnitude moving across and within distinct ecosystems. Similarly, C_{phyto}:POC ratios were variable with the lowest values coming from productive temperate waters and the highest from oligotrophic gyres. A strong relationship between C_{phyto} and b_{bp} is particularly significant because b_{bp} is a property retrievable from satellite ocean color measurements. Our results, therefore, are highly encouraging for the global monitoring of phytoplankton biomass from space. The continued application of our C_{phyto} measurement approach will enable validation of satellite retrievals and contribute to an improved understanding of environmental controls on phytoplankton biomass and physiology.

1. Introduction

The direct measurement of phytoplankton carbon (C_{phyto}) in the field has long been recognized as critical for understanding plankton dynamics (e.g. growth, production) in the marine environment (Sutherland, 1913; Eppley, 1968; Laws, 2013). Accurate estimates of C_{phyto} at local, regional, and global scales provide a means to observe phytoplankton standing stocks and seasonal or inter-annual biomass trends relative to environmental variability. Despite this ongoing need, the direct assessment of C_{phyto} has proven an elusive goal. Key to this challenge has been an inability to isolate phytoplankton from the pool of other particulate forms of carbon that are abundant in seawater (zooplankton, detritus, bacteria, etc.). Consequently, proxy measurements or conversions of properties related to phytoplankton have been heavily relied upon to evaluate C_{phyto}.

Historical biomass proxies have included cell counts (Sutherland, 1913), color indices (Reid et al., 1998), chlorophyll (Kreps and Verjbinskaya, 1930), adenosine triphosphate (ATP) (Sinclair et al., 1979), proportions of particulate organic carbon (Strickland, 1960), and cell volume (Strathmann, 1967; Verity et al., 1992; Montagnes et al., 1994), all of which require conversions to biomass estimates. Single cell elemental analysis (Heldal et al., 2003) has been performed and has potential, but thus far is very limited in the number of cells that have been analyzed from a sample. Some of the proxy estimates are uniquely tied to phytoplankton (e.g. cell counts, pigments) while others are clearly influenced by non-phytoplankton organisms and non-living seawater constituents (e.g. ATP, POC). Nevertheless, these estimates have greatly influenced our understanding of phytoplankton abundance and community dynamics, as well as the interpretation of long-term trends in phytoplankton properties (Reid et al., 1998; Mcquatters-Gollop et al., 2011). More thorough discussions of these proxies and their relationships with C_{phyto} can be found elsewhere (e.g. Banse, 1977; Geider et al., 1997; Graff et al., 2012).

A more recent alternative approach to assessing C_{phyto} has been through analyzing variability in light scattering properties, specifically the particulate beam attenuation coefficient (c_p) and the

* Corresponding author. Tel.: +1 541 737 5274.
E-mail address: jrgraff@science.oregonstate.edu (J.R. Graff).
[1] Current address: University of Technology Sydney, Plant Functional Biology & Climate Change Cluster, Sydney, Australia.

http://dx.doi.org/10.1016/j.dsr.2015.04.006

particulate backscatter coefficient (b_{bp}). An appealing aspect of this approach is that these light scattering properties can be continuously measured in situ (Behrenfeld and Boss, 2003, 2006; Huot et al., 2007) and b_{bp} can be retrieved from space (Behrenfeld et al., 2005; Siegel et al., 2005; Westberry et al., 2008). These optical properties have the additional important advantage that they vary with particle abundance but, unlike chlorophyll, do not register physiological variability associated with light and nutrient conditions (i.e., variability in cellular Chl:C ratios). However, a drawback of the optical indices of C_{phyto} is that a portion of the scattered light is due to non-algal particles. The severity of this issue has not been quantified because, like all the other C_{phyto} proxies, direct comparisons with analytical field measurements of biomass have not been possible.

A solution to the long standing C_{phyto} problem was introduced in Graff et al. (2012) where a method was described for isolating the phytoplankton community from field samples and then assessing C_{phyto} of the sorted sample through elemental analysis. The approach employs sorting flow-cytometry to identify phytoplankton and separate them from non-algal particles. As demonstrated in Graff et al. (2012), the resultant sorted sample is highly representative of the in situ phytoplankton community. Carbon measured in the sorted sample is converted to in situ C_{phyto} using a cell count ratio calculated from cell counts from the sorted and whole seawater samples. In the original report (Graff et al., 2012) only a small set of samples collected off the Oregon Coast were collected to demonstrate the field application of the approach.

Here, we report analytical measurements of C_{phyto} covering a diversity of open ocean conditions, ranging from Pacific and Atlantic oligotrophic gyres to equatorial upwelling systems and temperate waters. We compare our direct phytoplankton biomass estimates to simultaneous measurements of b_{bp}, c_p, Chl a concentration and total particulate organic carbon (POC). From this comparison, we provide a new parameterization for the relationship between C_{phyto} and b_{bp}, the latter property being the biomass proxy exhibiting the best correlation with C_{phyto}. The new relationship can be applied to satellite retrievals of b_{bp} and resultant C_{phyto} estimates employed, for example, in the Carbon-based Productivity Model (CbPM) (Westberry et al., 2008), to re-evaluate global variability in ocean net primary production. Validated assessments of C_{phyto} will also help discern underlying drivers of change (e.g. nutrients, light environment, etc.) in historical field and satellite chlorophyll records (Boyce et al., 2010, 2014; Siegel et al., 2013).

2. Material and methods

Field samples were collected during two cruises (Fig. 1). The first cruise took place in the Equatorial Pacific Ocean (EPO) in conjunction with the National Oceanic and Atmospheric Administration's (NOAA) Tropical Atmospheric Ocean (TAO) project aboard the NOAA Vessel Ka'imimoana from 7 May to 28 June 2012 (Fig. 1). The second field effort was part of the 22nd Atlantic Meridional Transect (AMT-22) on the RSS James Cook from 10 October to 24 November 2012 (Fig. 1). During each cruise, surface optical properties were continuously measured and discrete samples were collected for C_{phyto}, high-pressure liquid chromatography (HPLC) pigments and POC.

2.1. Analytical C_{phyto} measurements

Collection and elemental analyses of C_{phyto} samples, hereto referred to as direct or analytical C_{phyto}, were made following a modified procedure first described in Graff et al. (2012). Surface samples were collected from seawater flow-through lines on both cruises and from a Niskin rosette when possible on the EPO cruise. Comparative tests (data not shown here) were performed during the TAO cruise to compare samples collected using a Niskin and flow-through lines. No differences in the abundance or community composition of the samples were apparent. Samples for sorting and collecting phytoplankton cells were processed on a BD Biosciences Influx Cell Sorter (BD ICS) flow-cytometer. The BD ICS was aligned and calibrated for cell sorting before whole seawater was collected. Sample lines were flushed for approximately 30 min prior to sample collection and cell sorting to remove potential contamination from the fluorescent beads used for alignment and calibration and the detergents in which they are stored. Our BD ICS is equipped with a 488 nm (blue) excitation laser, fluorescence collection at 530 nm and 692 nm, side scatter detection, and forward scatter detection for resolving small particles (down to 0.2 μm). A 100 μm nozzle tip was used for all samples. Gates for selecting and sorting cells were drawn to select for the scatter and fluorescence signatures of all phytoplankton groups present in the samples. Up to 4 mL of whole seawater were sorted at sea for each sample. Sort times ranged from less than 1 h up to 4 h, resulting in 0.75–1 mL samples composed of sorted phytoplankton cells suspended in artificial sheath fluid (deionized water and sodium chloride) (Graff et al., 2012). A sample of sheath water was collected from the nozzle following each sort and used to correct carbon values for sorted samples for the dissolved organic contribution from the sheath fluid. All samples were immediately frozen in liquid nitrogen (LN) and stored at −80 °C or in LN until they were analyzed.

Analysis of sorted phytoplankton and sheath fluid samples was performed on a Shimadzu TOC-N analyzer using manual injection techniques. Manual injection methods require less volume compared to automated protocols, which use a portion of a sample for filling and rinsing the sample lines and syringe. Due to sample salinity, ceramic wool in the combustion column was replaced with platinum wire beads (Carlson et al., 2004). The Shimadzu TOC-N provides an integrated area under a response curve for each sample. The difference in area between the sorted phytoplankton sample and the sheath fluid is attributed to C_{phyto}. Each sample analyzed was first acidified to a pH < 2.0 and sparged for 10 min with 75 mL min^{-1} of ultra pure air to remove inorganic carbon. A minimum of three 100 μl replicate injections per sample were analyzed and the mean area was calculated using 2–3 of the replicates with the lowest coefficient of variation (average CV for field samples = 0.047). Instrument accuracy and precision were checked throughout the day and prior to sample analysis with deionized water and a seawater reference standard (~40–44 μmol L^{-1} carbon) from the Consensus Reference Materials Project hosted at the Hansell Lab at the University of Miami.

Phytoplankton carbon in the sorted sample was determined by subtracting the mean area of the sheath fluid sample from the mean area of the sorted phytoplankton sample and converting to biomass using the instrument calibration. The areas for the sheath samples (~18–20 μM) are generally half of the values obtained when analyzing the standard reference material and well above the detection limits of the instrument. Measured signals for sorted samples containing cells are higher than their paired sheath sample values. The additional signal area due to cells is a variable fraction of the sheath signal and is dependent upon the concentration and types of cells in the sorted sample. The low coefficient of variation for each sample (median = 0.04) provides the resolution required to determine the difference between the sheath and sorted samples. Cell counts for the whole seawater samples and for each sorted sample were determined on the BD ICS. In situ C_{phyto} was calculated by dividing the carbon attributed to the phytoplankton portion of the sorted sample by the cell concentration ratio between the sorted and natural samples (Graff et al., 2012). *Synechococcus* cell count ratios were used here as they are easily discernible as a group from both noise and other cell types based on fluorescence and scatter properties and were present in all samples.

To calibrate the Shimadzu TOC-N, natural phytoplankton were used as a standard material. Whole seawater was collected 25 miles

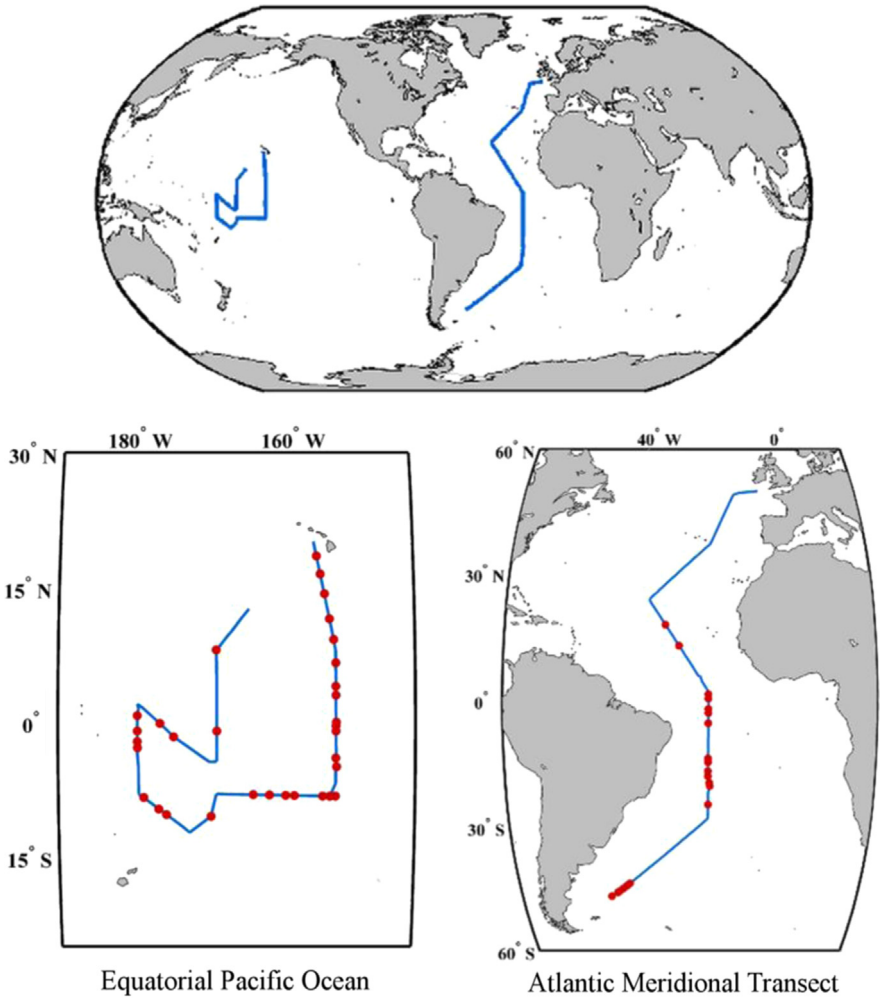

Fig. 1. (A) Cruise tracks for (B) the Equatorial Pacific Ocean (EPO) and (C) and the 22nd Atlantic Meridional Transect (AMT-22). Red circles indicate locations where samples for analytical phytoplankton carbon measurements were collected.

off the Oregon Coast on three separate cruises. Phytoplankton from each sample were sorted at Oregon State University on the BD-ICS for up to 7 h to obtain enough sample volume for TOC-N analysis and for filtration onto a pre-combusted 25 mm Whatman glass fiber filter (GF/F, combusted at 450 °C for 4 h). Sorted phytoplankton filters were analyzed on an Exeter Analytical CE-440 elemental analyzer following the protocol for POC analysis outlined below. Filters with cells (plus DOC) contained carbon ranging from 8.5 to 20 μg per filter. To obtain phytoplankton carbon values from the filters, GF/F carbon was corrected for the filter blank and dissolved organic carbon (DOC) adsorption (Morán et al., 1999; Cetinić et al., 2012).

To determine filter blank and DOC contributions to GF/F filters over the mass and volume range for sorted and filtered phytoplankton samples, 20 μm cellulose particles (Sigma-Aldrich) were suspended in 0.22 μm filtered artificial sheath medium and volumes ranging from 0.5 mL up to 1 L were filtered through pre-combusted GF/Fs. Cellulose particles of this size should be effectively retained by a GF/F filter with an effective pore size after combustion of <0.5 μm (Chavez et al., 1995). Cellulose has a carbon composition of 33% by mass. All filters were frozen and analyzed after acidification and desiccation as described below for POC samples. These results provided a measure of carbon above and beyond the known mass of cellulose that should be retained by the filter in the mass and volume ranges of the sorted phytoplankton filtered onto GF/Fs. A linear model was developed using the ratio of the carbon from the GF/F filters containing cellulose and the actual mass of the cellulose on the filter (i.e. GF/F carbon:cellulose carbon) regressed against the measured carbon mass of the GF/F. This provided a correction to apply to the sorted and filtered phytoplankton samples. The calibration was created using the corrected GF/F phytoplankton carbon values and the Shimadzu TOC-N area difference between the sorted phytoplankton and sheath fluid samples (calibration $R^2=0.98$).

2.2. Pigments and particulate organic carbon

For HPLC pigment samples, 1–3 L of whole seawater were filtered onto a pre-combusted GF/F. Each filter was immediately placed into a cryovial and stored in LN. Samples were analyzed at the NASA Goddard Space Flight Center Ocean Ecology Laboratory following established protocols (Van Heukelem and Thomas, 2001).

For POC samples, three volumes of 0.5 L, 1 L, and 2.135 L were filtered onto pre-combusted GF/F filters. Filters were wrapped in pre-combusted foil (450 °C, 4 h) and stored in LN until sample preparation and analysis. Prior to analysis, filters were fumed with hydrochloric acid for 4 h and then dried at 50 °C for 24 h. All POC filters were analyzed on an Exeter Analytics CE-440 elemental analyzer calibrated with acetanilide following manufacturer protocols. POC values reported here were corrected for non-target carbon from filter blanks and DOC adsorption.

At each station, two blank values were determined in order to correct POC measurements for non-target carbon. The blanks included (1) a 1 L sample of seawater retained from each 1 L POC

filtration and then re-filtered through a new pre-combusted GF/F and (2) an intercept blank from the regression of carbon values and volumes for three POC samples at each station. Tests were conducted to determine the relationship of dissolved organic carbon (DOC) adsorption with volume filtered. For these tests, multiple volumes, 0.01–3 L, of GF/F pre-filtered Equatorial Pacific and Oregon Coastal seawater re-filtered through pre-combusted GF/F filters. All filters were frozen in LN and analyzed after acidification and desiccation as described above.

Results from the natural pre-filtered seawater tests showed that DOC adsorption was linear with volume, with no saturation observed up to 3 L. As such, a linear approach was taken in order to correct each multi-volume set of field POC samples. For each station, a linear regression between POC values and volume provided a *y*-intercept blank that represents a filter that has been handled but has not been used for filtration. The 1 L blank value for pre-filtered seawater at each station represents DOC adsorption to a GF/F specific for that water source. Thus, a linear model between the *y*-intercept and the 1 L blank sample represents the filter blank plus a linear dependence of DOC adsorption. We used this approach to determine the non-target carbon contribution for each volume filtered at each station and subtracted this from the corresponding POC filter value. The method accounts for variable DOC constituents and their adsorption to a GF/F specific at each station where the sample was collected.

2.3. Optical properties

Optical parameters were continuously measured on the flow-through seawater systems of both research vessels using 2 WETLabs ECO-BB3 backscattering sensors (470 × 2, 532 × 2, 595, and 656 nm) mounted in custom-made backscattering flow chambers (Dall'Olmo et al., 2009), 2C-star transmissometers (532 and 660 nm), and 1 WETLabs AC-s hyperspectral absorption and attenuation meter. Optical seawater blanks, which were used to remove the non-particulate portion of the optical signals, were collected by switching the flowing seawater through a 0.22 μm filter using an automatic valve-switch and controller (Slade et al., 2010). Particulate backscattering at 470 nm (b_{bp}) from the ECO-BB3 and particulate beam attenuation at 660 nm (c_p) from a C-star transmissometer were calculated following Dall'Olmo et al. (2009). Values reported here represent an average for 3–60 min centered at the time of sample collection for analytical measurements of C_{phyto}, pigments, and POC. Shorter time averages were used in temperate waters where heterogeneity in particle fields resulted in extremely high variability in each parameter over longer time scales, and thus distances, while underway. Growth irradiance (E_g (mol quanta m^{-2} s^{-1})) values were calculated from the daily noon CTD casts as the median mixed layer light level following Behrenfeld et al. (2005) and interpolated between casts to estimate E_g where samples were collected.

3. Results

Fifty-three C_{phyto} samples were collected and analyzed for the two cruises, 32 of which were from the EPO cruise and 21 from AMT-22 (Fig. 1B and C, red circles). The C_{phyto} samples were from distinct oceanographic regions traversed during the two cruises, ranging from oligotrophic gyres to temperate spring conditions in the southern hemisphere. POC and HPLC samples were collected at a total of 302 stations, with 107 from the EPO cruise and 195 from AMT-22.

3.1. Analytical and optical measurements

For AMT-22, analytical C_{phyto} values ranged from 4 to 58 μg L^{-1} (Table 1), with the lowest values observed in the South Atlantic subtropical gyre and the highest biomass observed in the austral-spring South Atlantic temperate waters. Measured C_{phyto} values for the EPO cruise were more constrained than in the Atlantic, ranging from 5 μg L^{-1} in the North Pacific gyre to 35 μg L^{-1} in the equatorial upwelling zone (Table 1). Particulate organic carbon ranged from 9 to 229 μg L^{-1} for the two cruises, while HPLC Chl a ranged from 0.026 to 1.13 μg L^{-1} (Table 1). As with C_{phyto}, a smaller range in POC and HPLC values was observed during the EPO cruise (Table 1). The ratio of C_{phyto}:Chl a ranged from 31 to 358 with a median of 101. The highest C_{phyto}:Chl a values were found in oligotrophic gyres and the lowest values in equatorial upwelling and temperate waters. Particulate backscattering coefficients exhibited the largest range during AMT-22, spanning from 0.46×10^{-3} to 3.8×10^{-3} (Table 1 and Fig. 2C and F).

Table 1
Ranges of analytical phytoplankton carbon and associated parameters measured in the Equatorial Pacific Ocean (EPO) and during the 22nd Atlantic Meridonal Transect cruise (AMT-22). C_{phyto}=phytoplankton carbon, POC=particulate organic carbon, HPLC Chl a=high-pressure liquid chromatography chlorophyll a, b_{bp}=particulate backscattering coefficient.

Parameter	Range of measured values		
	All (N=53)	EPO (N=32)	AMT-22 (N=21)
C_{phyto} (μg L^{-1})	4–58	5–35	4–58
POC (μg L^{-1})	9–229	9–97	9–229
HPLC Chl a (μg L^{-1})	0.026–1.13	0.05–0.75	0.026–1.13
$b_{bp\ 470}$ (m^{-1})	0.00046–0.0038	0.00077–0.0025	0.00046–0.0038

3.2. Regression analyses

Analytical C_{phyto} measurements exhibited a strong linear relationship with particulate backscattering coefficients (b_{bp}) (Fig. 3 and Table 2), with b_{bp} explaining nearly 70% of the variability in phytoplankton carbon (R^2=0.69, root mean square error (RMSE)=4.6, $p \ll 0.05$). Chlorophyll a had a positive, but weaker, relationship with C_{phyto} (R^2=0.52, RMSE=5.1, $p \ll 0.05$) (Fig. 4A and Table 2). Particulate organic carbon also had a positive but weaker relationship with C_{phyto} (R^2=0.52, RMSE=5.1, $p \ll 0.05$) (Fig. 4B and Table 2). An even weaker relationship was observed between phytoplankton biomass and c_p (R^2=0.42, RMSE=5.8, $p \ll 0.05$) (Fig. 5B and Table 2), whereas POC showed a very strong relationship with c_p (R^2=0.92, $p \ll 0.05$) (Fig. 5C).

3.3. Optically derived C_{phyto}

The relationship between C_{phyto} and b_{bp} (Fig. 3) was applied to our continuous underway measurements of b_{bp} (470 nm) to allow for a more extensive evaluation of phytoplankton biomass variability in the study regions. This analysis yielded a total range for C_{phyto} of 10–31 μg L^{-1} and 6–46 μg L^{-1} for the EPO and AMT-22 cruises, respectively (Table 1). A relationship between b_{bp} at 470 nm and C_{phyto} is not dependent a priori on the use of blue light as a biomass proxy. The slope of b_{bp} across the visible spectrum is generally invariant (Stramski and Kiefer, 1991) and it may be possible to construct a similarly strong relationship with other wavelenths of particulte backscattering coefficients. However, 470 nm is close to that retrieved by current satellite technologies (443 nm), and thus, more readily comparable and evaluated for its global application.

Focusing on the AMT-22 cruise, C_{phyto}:Chl a ratios ranged from 35 to 408 with a median of 99 (Fig. 6). Phytoplankton biomass (Fig. 7B) accounted for 12–97% of POC (Fig. 7A), with an average of 44% (Fig. 7C). Looking more closely at previously defined regions along this transect (Robinson et al., 2006), we find that C_{phyto} makes the greatest contribution to POC in the oligotrophic gyres (i.e., 'N. Gyre' and 'S. Gyre' in Fig. 7C), while being a smaller faction of POC in the equatorial region and in the more southern temperate waters of the South Atlantic (i.e., 'Equatorial' and 'S. Temp' in Fig. 7C).

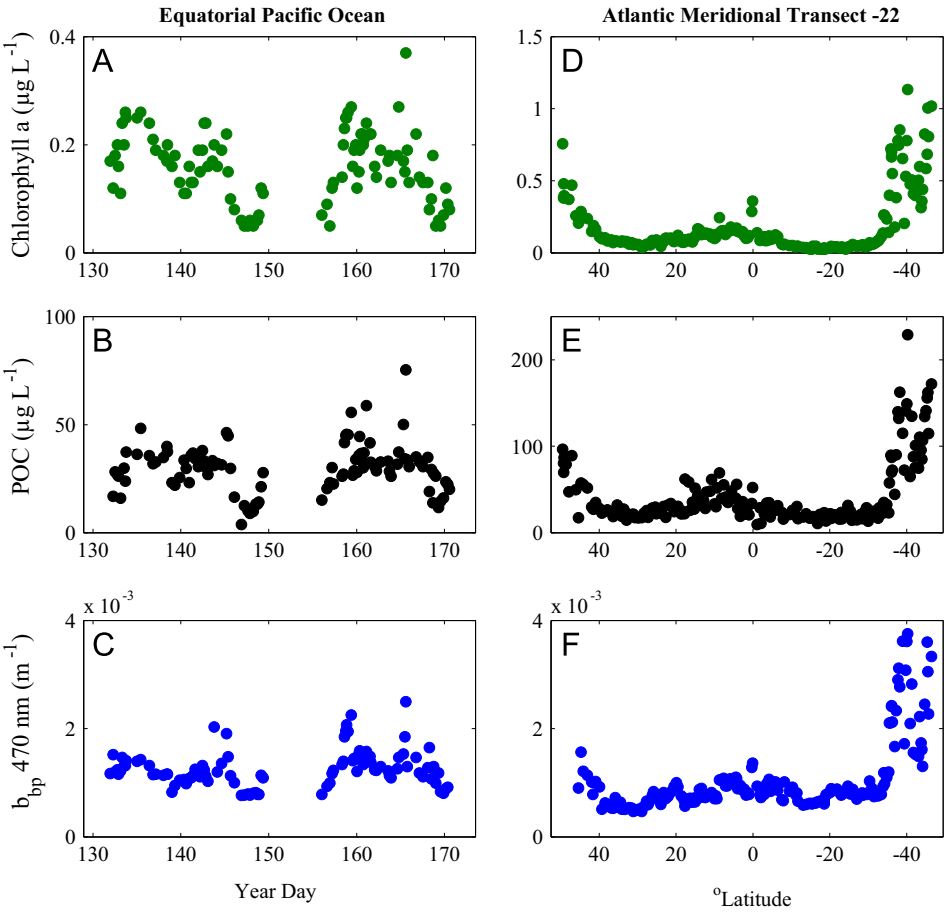

Fig. 2. Transect data for the EPO (A–C) and AMT-22 cruises (D–F) of HPLC Chl a (A, D), particulate organic carbon (POC) (B, E), and the particulate backscattering coefficient (b_{bp} at 470 nm) (C, F).

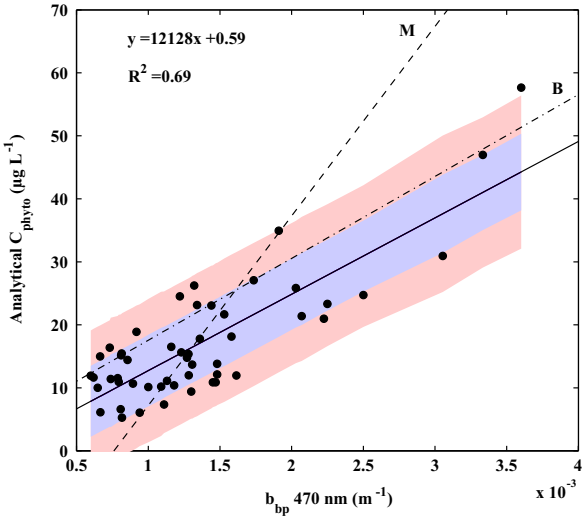

Fig. 3. Regression analysis of analytically derived phytoplankton carbon (C_{phyto}) with the particulate backscattering coefficient (b_{bp}), R^2=0.69. Confidence intervals of prediction of 68% (blue) and 95% (red) are shown for the regression. Previously published relationships from Behrenfeld et al. (2005) (-.-. B, y=13,000x+4.55) and Martinez-Vicente et al. (2013) (- - M, y=30,100x−22.9) are provided for comparison.

4. Discussion

Here, we report direct measurements of C_{phyto} for the open ocean. These data span an order of magnitude, with the highest biomass samples collected from temperate South Atlantic waters, followed by equatorial upwelling regions, and the lowest values found in oligotrophic gyres. These direct measurements of C_{phyto} allow evaluation of phytoplankton standing stocks relative to environmental conditions and independent of changes in intercellular chlorophyll or methodological inconsistencies (e.g. C_{phyto}:volume ratio). For example, field values of C_{phyto}:Chl a ratios exhibited high variability and ranged from 31 to 358 (Fig. 6A, black circles). Future measurements at high latitudes and in coastal upwelling regions may extend this range in C_{phyto}:Chl a. For this dataset alone, applying a single conversion factor between chlorophyll and phytoplankton carbon for this dataset would have resulted in up to 3-fold under- or overestimates of C_{phyto} for large parts of the ocean.

Table 2
Regression analyses of direct measurements of phytoplankton carbon (C_{phyto}) with proxy biomass measurements of HPLC Chl a, POC, and optical parameters. All regressions were significant with p-values≪0.05. C_{phyto}=phytoplankton carbon, b_{bp}=particulate backscattering coefficient, HPLC Chl a=high-pressure liquid chromatography chlorophyll a, POC=particulate organic carbon, c_p=beam attenuation coefficient.

Proxy Measurement	Regression analysis with C_{phyto}			
	Slope	Intercept [a]	R^2	RMSE [a]
$b_{bp\ 470}$ (m^{-1})	12,128	0.59	0.69	4.6
HPLC Chl a (μg L^{-1})	33.7	9.7	0.52	5.1
POC (μg L^{-1})	0.189	8.7	0.52	5.1
c_p (m^{-1})	74.2	11	0.42	5.8

[a] Intercept and RMSE in units of μg C L^{-1}.

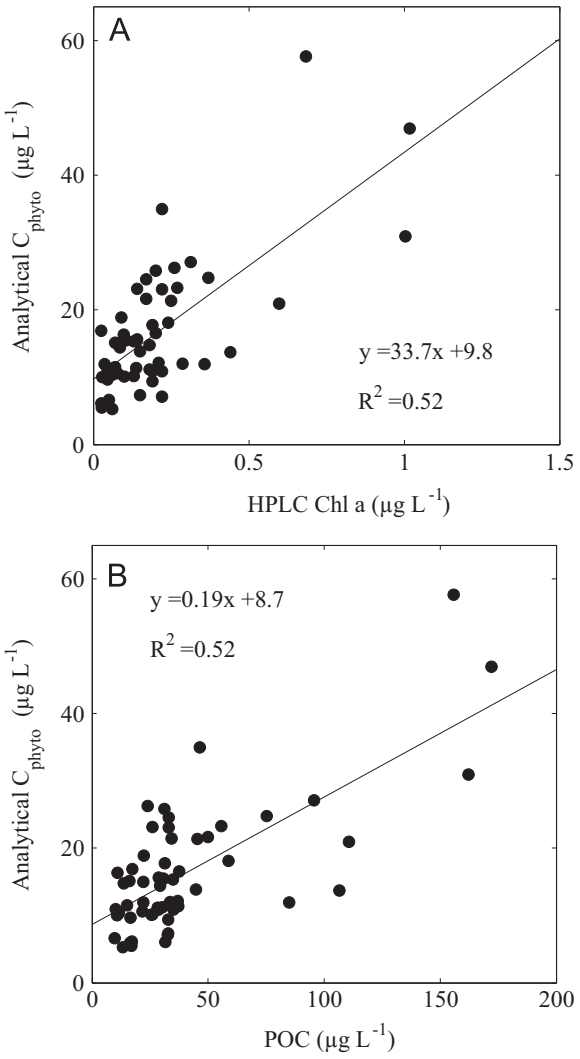

Fig. 4. Regression analyses of analytical measurements of (A) HPLC Chl a and C_{phyto} and (B) POC and C_{phyto}. Both regressions resulted in an R^2=0.52.

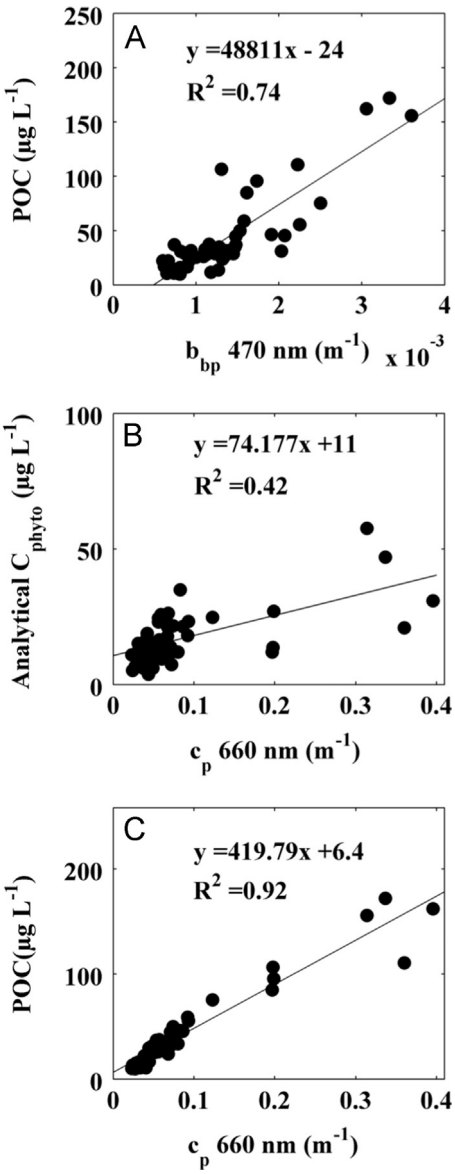

Fig. 5. Regression analyses of (A) POC and b_{bp}, (B) C_{phyto} and c_p, and (C) POC and c_p.

Over the range of biomass samples in this dataset, C_{phyto} is linearly related to the particulate backscattering coefficient (b_{bp}) (R^2=0.69, Fig. 3 solid line) where C_{phyto}=12,128 × b_{bp}+0.59 (Fig. 3). The relationship between b_{bp} and C_{phyto} differs strongly from that of Martinez-Vicente et al. (2013) (dashed line in Fig. 3), which was derived by converting flow cytometry-based phytoplankton cell volumes to biomass. Volume based phytoplankton biomass conversions rely upon the assumed C_{phyto}:volume relationship(s) (Verity et al., 1992; Montagnes et al., 1994; Menden-Deuer and Lessard, 2000). The range in published values for this ratio can yield an order of magnitude variability in resultant C_{phyto} estimates (Caron et al., 1995; Dall'Olmo et al., 2011). Despite the quantitative difference between our results and those of Martinez-Vicente et al. (2013), a qualitative consistency between these two studies is that b_{bp} and C_{phyto} are significantly correlated. The results of this field study yielded a slope for the b_{bp} to C_{phyto} relationship (i.e., 12,128 µg L^{-1} m^{-1}) that is nearly identical to that in Behrenfeld et al. (2005) of 13,000 µg L^{-1} m^{-1}. This latter study was based entirely on analyses of satellite data for b_{bp} at 443 nm. While the wavelength analyzed differs between this study and that of Behrenfeld et al. (2005), this discrepancy would only result in a small percentage difference in b_{bp} values. An important deviation between the current results and those of Behrenfeld et al. (2005) is the lower intercept for our b_{bp} and C_{phyto} relationship (0.59 vs. 4.55, compare solid and dot-dash lines in Fig. 3). The differences in intercept and slope between these equations would imply that C_{phyto} estimates in the earlier study were overestimated, if only slightly. A slight bias (high) in satellite b_{bp} retrievals could be the basis for this difference in intercept. This possibility emphasizes that, in terms of global biomass assessments, a critical need still exists for increasing field validation data for both C_{phyto} and b_{bp}. Particulate organic carbon (PIC) also influences measurements of b_{bp} (Balch et al., 2010) and may lead to increased error around the relationship or overestimations of C_{phyto} using the existing model. Coccolithophores are a small background component of the phytoplankton community and are inherently included in the b_{bp} vs. C_{phyto} regressions (Fig. 1). When they are a small component of the community they likely add to the error around the derived relationship. However, locally significant increases in PIC or blooms of calcifying organisms should be considered carefully in future evaluations and applications of the b_{bp} vs. C_{phyto} relationship.

Our regression of direct C_{phyto} measurements and Chl has a positive y-intercept (Fig. 4A and Table 2). This positive intercept is unlikely due to unaccounted for carbon contamination in the samples. Rather, as the result of photoacclimation and nutrient driven changes in intercellular pigmentation, one should expect a non-zero intercept between Chl and biomass in a study spanning a wide range of environmental parameters where an order of

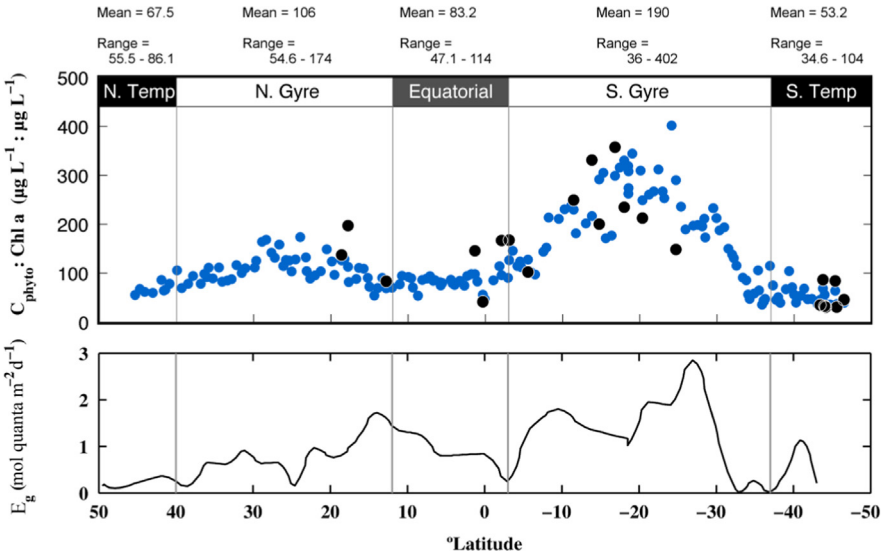

Fig. 6. Transect data from AMT-22 for C_{phyto}:Chl a ratios from direct measurements of C_{phyto} (black circles) and optically derived from $b_{bp\ 470}$ (blue circles) using the new relationship (Fig. 3 solid line).

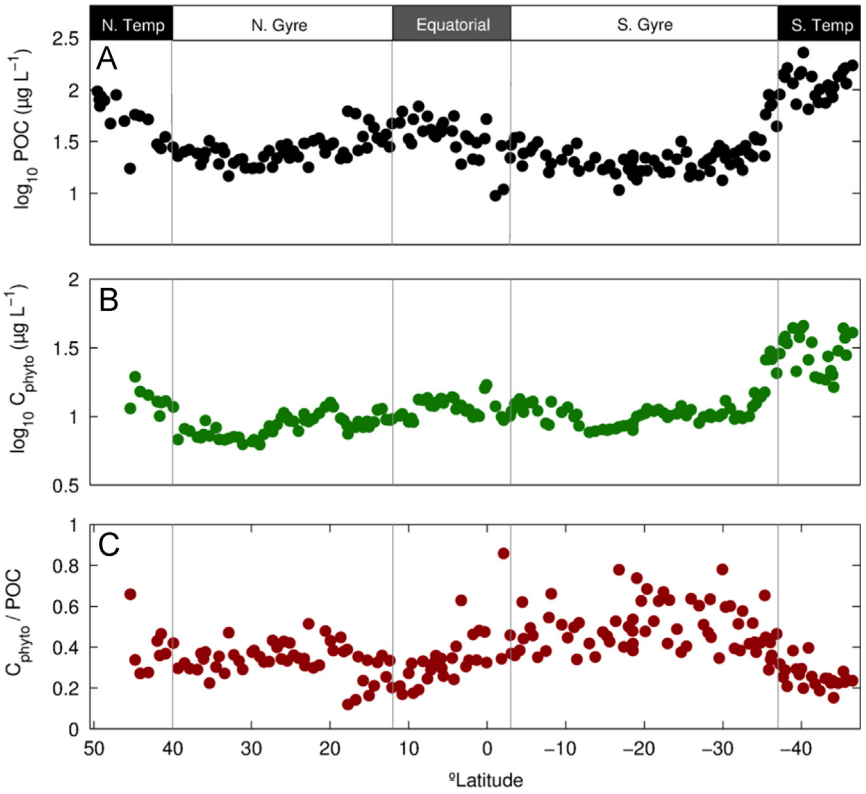

Fig. 7. AMT-22 transect data of (A) POC, (B) optically derived C_{phyto} using the relationship in Fig. 3, and (C) the ratio of C_{phyto} to POC. Note log scale for A and B.

magnitude change in Chl can be associated with the same biomass. A regression of whole water total phytoplankton cell counts from our study with Chl also results in a significant positive intercept of 7×10^9 cells. If we conservatively assume that all of these cells are *Prochlorococcus* in these high-light low-chlorophyll waters and apply a nominal value of 100 fg C cell^{-1}, from a reported range of 35 (Veldhuis and Kraay, 2004) to 350 (Caron et al., 1995 and references therein), this intercept is approximately 7 µg C L^{-1}. Converting cell counts to carbon are, of course, subject to a wide range of conversion factors applied to different cells types that would significantly impact the regression of C_{phyto} and Chl and the resulting intercept. For comparison, an analysis of published data aimed at determining planktonic carbon contributions to total POC (Caron et al., 1995) resulted in an intercept of 5.0 µg C L^{-1}. A more rudimentary approach, and one commonly applied to obtain phytoplankton biomass estimates, is to multiply the chlorophyll values by a C_{phyto}:Chl (Θ) conversion factor. If we divide our samples based on Chl values above and below 0.25 µg L^{-1}, a value that delineates open ocean gyres from temperate waters in our dataset. Applying Θ values which are representative of gyre conditions (Θ=90) and temperate waters (Θ=30) (Riemann et al., 1989; Sherr et al., 2005) the same regression analysis results in an intercept of 6.7 µg C L^{-1}. Lastly, any loss of small cells and/or pigments when filtering through GF/Fs (Taguchi and Laws, 1988; Stockner et al., 1990; Dickson and Wheeler, 1993; Nayar and Chou, 2003; Knefelkamp et al., 2007) would also confound this analysis, shifting the relationship towards a higher *y*-

intercept by shifting chlorophyll values for samples with small cells to lower chlorophyll values. Thus, the results of our analysis are not unusual and only serve to emphasize the point that Chl is not the best estimator of biomass.

We find that chlorophyll and POC concentrations exhibit weaker relationships with C_{phyto} than that observed for b_{bp} (Fig. 4A and B). Cellular chlorophyll concentration is strongly influenced by photoacclimation (i.e. changes in pigmentation in response to changes in growth irradiance) and nutrient-driven growth rate (Geider et al., 1997; Behrenfeld et al., 2005). Accordingly, the capacity to routinely measure C_{phyto} and Chl a simultaneously in the field represents a new opportunity to decipher and understand Chl:C_{phyto} variability in natural phytoplankton assemblages. Similarly, POC is not solely a function of phytoplankton biomass, but also registers non-algal particulate matter (Banse, 1977). Thus, simultaneous measurements of C_{phyto} and POC can contribute to improved understanding of factors controlling trophic level carbon balances in marine ecosystems.

In the current investigation using direct measurements of phytoplankton biomass, there is a closer relationship between direct measurements of C_{phyto} and b_{bp} than for C_{phyto} and c_p (Figs. 3 and 5B). Previous studies have found tight correlations with both of these optical indices and proxy estimates of C_{phyto} (DuRand and Olson, 1996; Claustre et al., 1999; Behrenfeld and Boss, 2006). The particulate beam attenuation coefficient (c_p), in theory, is most sensitive to particles in the size range of the majority of phytoplankton (0.5–20 μm) while smaller particles are thought to dominate the b_{bp} signal (Stramski and Kiefer, 1991). Thus, we were somewhat surprised by the weaker relationship between C_{phyto} and c_p. However, it is noteworthy that the correlation coefficient for this relationship is significantly influenced by a relatively small number of samples that have high POC values from the temperate South Atlantic. As discussed below, these springtime conditions were potentially supporting an enhanced grazing community relative to phytoplankton concentration that was being detected in measurements of c_p but not b_{bp}. While b_{bp} is supposed to be most sensitive to small spherical particles, phytoplankton have more complex shapes and internal components and backscatter light more efficiently than theory would predict for perfect spheres (Meyer, 1979; Kitchen and Zaneveld, 1992; Vaillancourt et al., 2004; Clavano et al., 2007).

With respect to future field measurements of C_{phyto}, a cautionary note is needed regarding samples containing very large cells, particularly chain-forming phytoplankton species (e.g. *Chaetoceros* species). These cells are difficult (at best) to sort using a BD ICS. Consequently, assessments of C_{phyto} need to include an additional measurement for quantifying the carbon contribution of very large cells (e.g. hand sorted cell collection, imaging flow-cytometry (Olson and Sosik, 2007), microscopic enumeration) when such species are abundant (e.g., open ocean blooms, coastal upwelling areas, nearshore regions, estuaries). With respect to the current study, it is very unlikely that our C_{phyto} values are biased by unaccounted for large phytoplankton. During AMT-22, samples were collected at 20 m depth in the temperate southern region (i.e., the area of highest production for our field studies) and analyzed with a FlowCam. These measurements indicated that the average cell diameter for the largest cells, which were diatoms and dinoflagellates, was 34.5 μm (E. Fileman, Plymouth Marine Labs, personal communication). The set-up for our BD-ICS for these cruises used a 100 μm diameter sort nozzle and thus was able to sort cells in this size class.

Application of the C_{phyto} to b_{bp} relationship for the AMT-22 cruise extends our C_{phyto} observations along the transect. Ratios of C_{phyto}:Chl a calculated using optically derived C_{phyto} exhibit an order of magnitude range (35–408, median = 99) (Fig. 6A, green circles). While much of this range can be attributed to changes in intercellular pigments due to growth irradiance (E_g) differences between similar light environments are also apparent. For example, 25°N and 35°S have similar E_g values (~ 0.2 mol quanta m^{-2} s^{-1}) yet very different C_{phyto}:Chl a ratios, approximately 35 and 110 respectively, possibly reflecting differences in nutrient availability. There are dramatic trends in this ratio even within an environment like the South Atlantic oligotrophic gyre (Fig. 6A, S. Gyre). This variability illustrates the potential error associated with extracting C_{phyto} estimates from Chl a data.

Another interesting relationship observed during AMT-22 was the latitudinal pattern in the C_{phyto}:POC ratio (Fig. 7C). Regions with the highest C_{phyto} and highest net primary production (i.e. Equatorial Upwelling and temperate Spring waters) exhibited C_{phyto}:POC values that rarely exceeded 40% (average ~ 25%). This observation contrasts with enhanced biomass at coastal upwelling sites where phytoplankton can dominate POC (Hobson et al., 1973). A low contribution of C_{phyto} to POC in productive offshore waters, however, is consistent with the studies of Andersson and Rudehäll (1993) and Hobson et al. (1973), which included peak bloom conditions in a coastal region (Hobson et al., 1973; Andersson and Rudehäll, 1993). These differences between environments reflect system variability in producer and consumer dynamics, processes influencing the particle field, and possibly the export efficiency of different particle types. The substantial variability in C_{phyto}:POC values documented in these studies and illustrated in Fig. 7C illustrates the potential for significant error when extracting C_{phyto} estimates from POC.

The absence of analytical C_{phyto} measurements in the field has resulted in a prolonged reliance on proxies with tentative relationships to phytoplankton biomass, in particular chlorophyll concentration. Historical in situ and satellite records of chlorophyll have been used to evaluate trends and draw conclusion on phytoplankton biomass and its relation to climate forcings (e.g. Boyce et al., 2010, 2014; McQuatters-Gollop et al., 2011). The recent assessment of C_{phyto} from satellite b_{bp} (Behrenfeld et al., 2005; Westberry et al., 2008) has allowed a re-evaluation of chlorophyll variability, with some important conclusions. In particular, such studies have shown that temporal changes in chlorophyll over large ocean regions can be predominantly due to physiologically-driven modifications in cellular Chl:C ratios, rather than changes in biomass (Behrenfeld et al., 2005, 2009; Siegel et al., 2013). These findings have strong implications regarding ecosystem trophic dynamics, carbon export, and assessments of change in net primary production. However, confidence in these results has been hampered by a lack of validation data for evaluating the satellite C_{phyto} retrievals. Results presented here represent a first step in this validation (Fig. 3). We strongly endorse the continued application of this C_{phyto} measurement approach in future field studies, particularly in concert with paired measurements of pigment concentration and POC, to both improve global assessments of phytoplankton biomass and to allow more detailed in situ investigations of phytoplankton physiology and its relation to environmental variability.

Advances in technology (sorting flow-cytometery, high-sensitivity elemental analyses) have allowed quantitative assessment of a key ocean ecosystem property, C_{phyto}, that has historically been impossible. Direct C_{phyto} measurements reported here and elsewhere (Casey et al., 2013) have (Martiny et al., 2013; Wallhead et al., 2014) and will continue to be applied to evaluate phytoplankton biomass and physiology on multiple spatial and temporal scales. It will be important to continue testing and improving the measurement approach and building toward a more extensive set of field data, particularly in high biomass waters. In the meantime, the strong relationship reported here between b_{bp} and C_{phyto} provides a path for exploring local-to-global scale phytoplankton carbon distributions at high spatial and temporal resolution using in situ and satellite optical measurements.

Acknowledgments

This work was funded by NASA Grant NNX10AT70G to M. Behrenfeld. We would like to thank the NOAA Tropical

Atmospheric Ocean Program and LCDR Brian Lake and the 22nd Atlantic Meridional Transect Program and the Principal Scientist Glen Tarran for providing field support to carry out this research. This study is a contribution to the international IMBER project and was supported by the UK Natural Environment Research Council National Capability funding to Plymouth Marine Laboratory and the National Oceanography Centre, Southampton. This is contribution number 259 of the AMT program.

References

Andersson, A., Rudehäll, A., 1993. Proportion of plankton biomass in particulate organic carbon in the northern Baltic Sea. Mar. Ecol. Prog. Ser. 95, 133–139.
Balch, W.M., Bowler, B.C., Drapeau, D.T., Poulton, A.J., Holligan, P.M., 2010. Biominerals and the vertical flux of particulate organic carbon from the surface ocean. Geophys. Res. Lett. 37, L22605.
Banse, K., 1977. Determining the carbon-to-chlorophyll ratio of natural phytoplankton. Mar. Biol. 41, 199–212.
Behrenfeld, M.J., Boss, E., 2003. The beam attenuation to chlorophyll ratio: an optical index of phytoplankton physiology in the surface ocean? Deep-Sea Res. Part I 50, 1537–1549.
Behrenfeld, M.J., Boss, E., 2006. Beam attenuation and chlorophyll concentration as alternative optical indices of phytoplankton biomass. J. Mar. Res. 64, 431–451.
Behrenfeld, M.J., Boss, E., Siegel, D.A., Shea, D.M., 2005. Carbon-based ocean productivity and phytoplankton physiology from space. Glob. Biogeochem. Cycle, 19. http://dx.doi.org/10.1029/2004GB002299.
Behrenfeld, M.J., et al., 2009. Satellite-detected fluorescence reveals global physiology of ocean phytoplankton. Biogeoscience 6, 779–794.
Boyce, D.G., Lewis, M.R., Worm, B., 2010. Global phytoplankton decline over the past century. Nature 466, 591–596.
Boyce, D.G., Down, M., Lewis, M.R., Worm, B., 2014. Estimating global chlorophyll changes over the past century. Progr. Oceanogr. 122, 163–173. http://dx.doi.org/10.1016/j.pocean.2014.01.004.
Carlson, C.A., Giovannoni, S.J., Hansell, D.A., Goldberg, S.J., Parsons, R., Vergin, K., 2004. Interactions between DOC, microbial processes, and community structure in the mesopelagic zone of the northwestern Sargasso Sea. Limnol. Oceanogr. 49, 1073–1083.
Caron, D.A., et al., 1995. The contribution of microorganisms to particulate carbon and nitrogen in surface waters of the Sargasso Sea near Bermuda. Deep-Sea Res. I 42, 943–972.
Casey, J.R., Aucan, J.P., Goldberg, S.R., Lomas, M.W., 2013. Changes in partitioning of carbon amongst photosynthetic pico- and nano-plankton groups in the Sargasso Sea in response to changes in the North Atlantic Oscillation. Deep-Sea Res. II 93, 58–70.
Cetinić, I., Perry, M., Briggs, N., Kallin, E., D'Asaro, E., Lee, C., 2012. Particulate organic carbon and inherent optical properties during 2008 North Atlantic Bloom Experiment. J. Geophys. Res. – Oceans 117, C06028. http://dx.doi.org/10.1029/2011JC007771.
Chavez, F.P., et al., 1995. On the Chlorophyll a Retention Properties of Glass-Fiber GF/F Filters. Limnol. Oceanogr. 40, 428–433.
Claustre, H., Morel, A., Babin, M., Cailliau, C., Marie, D., Marty, J.C., Tailliez, D., Vaulot, D., 1999. Variability in particle attenuation and chlorophyll fluorescence in the tropical Pacific: scales, patterns, and biogeochemical implications. J. Geophys. Res.: Oceans 104, 3401–3422.
Clavano, W.R., Boss, E., Karp-Boss, L., 2007. Inherent optical properties of non-spherical marine-like particles – from theory to observation. In: Gibson, R.N., Atkinson, R.J.A., Gordon, J.D.M. (Eds.), Oceanography and Marine Biology: An Annual Review, vol. 45. CRC Press - Taylor & Francis Group, pp. 1–38.
Dall'Olmo, G., Westberry, T.K., Behrenfeld, M.J., Boss, E., Slade, W.H., 2009. Significant contribution of large particles to optical backscattering in the open ocean. Biogeoscience 6, 947–967.
Dall'Olmo, G., et al., 2011. Inferring phytoplankton carbon and eco-physiological rates from diel cycles of spectral particulate beam-attenuation coefficient. Biogeoscience 8, 3423–3439.
Dickson, M.-L., Wheeler, P.A., 1993. Chlorophyll a concentrations in the North Pacific: does a latitudinal gradient exist? Limnol. Oceanogr. 38, 1813–1818.
DuRand, M.D., Olson, R.J., 1996. Contributions of phytoplankton light scattering and cell concentration changes to diel variations in beam attenuation in the equatorial Pacific from flow cytometric measurements of pico-, ultra-and nanoplankton. Deep-Sea Res. Part II 43, 891–906.
Eppley, R.W., 1968. An incubation method for estimating the carbon content of phytoplankton in natural samples. Limnol. Oceanogr 13, 574–582.
Geider, R., MacIntyre, H., Kana, T., 1997. Dynamic model of phytoplankton growth and acclimation: responses of the balanced growth rate and the chlorophyll a: carbon ratio to light, nutrient-limitation and temperature. Mar. Ecol. Prog. Ser. 148, 187–200.
Graff, J.R., Milligan, A.J., Behrenfeld, M.J., 2012. The measurement of phytoplankton biomass using flow-cytometric sorting and elemental analysis of carbon. Limnol. Oceanogr. – Methods 10, 910–920.
Heldal, M., Scanlan, D., Norland, S., Thingstad, F., Mann, N., 2003. Elemental composition of single cells of various strains of marine *Prochlorococcus* and *Synechococcus* using X-ray microanalysis. Limnol. Oceanogr. 48, 1732–1743.
Hobson, L., Menzel, D., Barber, R., 1973. Primary productivity and sizes of pools of organic carbon in the mixed layer of the ocean. Mar. Biol. 19, 298–306.
Huot, Y., Brown, C.A., Cullen, J.J., 2007. Retrieval of phytoplankton biomass from simultaneous inversion of reflectance, the diffuse attenuation coefficient, and Sun-induced fluorescence in coastal waters. J. Geophys. Res. Oceans 112, C06013. http://dx.doi.org/10.1029/2006JC003794.
Kitchen, J.C., Zaneveld, J.R.B., 1992. A three-layered sphere model of the optical properties of phytoplankton. Limnol. Oceanogr. 37, 1680–1690.
Knefelkamp, B., Carstens, K., Wiltshire, K.H., 2007. Comparison of different filter types on chlorophyll-a retention and nutrient measurements. J. Exp. Mar. Biol. Ecol. 345, 61–70.
Kreps, E., Verjbinskaya, N., 1930. Seasonal changes in the phosphate and nitrate content and in hydrogen ion concentration in the Barents Sea. J. Conseil 5, 329–346.
Laws, E.A., 2013. Evaluation of in situ phytoplankton growth rates: a synthesis of data from varied approaches. Annu. Rev. Mar. Sci. 5, 247–268.
Martinez-Vicente, V., Dall'Olmo, G., Tarran, G., Boss, E., Sathyendranath, S, 2013. Optical backscattering is correlated with phytoplankton carbon across the Atlantic Ocean. Geophys. Res. Lett. 40, 1154–1158.
Martiny, A.C., Pham, C.T.A., Primeau, F.W., Vrugt, J.A., Moore, J.K., Levin, S.A., Lomas, M.T., 2013. Strong latitudinal patterns in the elemental ratios of marine plankton and organic matter. Nat. Geosci. 6, 279–283.
McQuatters-Gollop, A., et al., 2011. Is there a decline in marine phytoplankton? Nature 472, E6–E7.
Menden-Deuer, S., Lessard, E.J., 2000. Carbon to volume relationships for dinoflagellates, diatoms, and other protist plankton. Limnol. Oceanogr. 45, 569–579.
Meyer, R.A., 1979. Light scattering from biological cells: dependence of backscatter radiation on membrane thickness and refractive index. Appl. Opt. 18, 585–588.
Montagnes, D.J., Berges, J.A., Harrison, P.J., Taylor, F., 1994. Estimating carbon, nitrogen, protein, and chlorophyll a from volume in marine phytoplankton. Limnol. Oceanogr. 39, 1044–1060.
Morán, X.A., Gasol, J.M., Arin, L., Estrada, M., 1999. A comparison between glass fiber and membrane filters for the estimation of phytoplankton POC and DOC production. Mar. Ecol. Prog. Ser. 187, 31–41.
Nayar, S., Chou, L., 2003. Relative efficiencies of different filters in retaining phytoplankton for pigment and productivity studies. Estuar. Coast. Shelf Sci. 58, 241–248.
Olson, R.J., Sosik, H.M., 2007. A submersible imaging-in-flow instrument to analyze nano-and microplankton: imaging FlowCytobot. Limnol. Oceanogr. – Methods 5, 195–203.
Reid, P.C., Edwards, M., Hunt, H.G., Warner, A.J., 1998. Phytoplankton change in the North Atlantic. Nature 391 546–546.
Riemann, B., Simonsen, P., Stensgaard, L., 1989. The carbon and chlorophyll content of phytoplankton from various nutrient regimes. J. Plankton Res. 11, 1037–1045.
Robinson, C., Poulton, A.J., Holligan, P.M., Baker, A.R., Forster, G., Gist, N., Jickells, T.D., Malin, G., Upstill-Goddard, R., Williams, R.G., Woodward, E.M.S., Zubkov, M.V., 2006. The Atlantic Meridional Transect (AMT) Programme: a contextual view 1995–2005. Deep-Sea Res. II 53, 1485–1515.
Siegel, D., et al., 2013. Regional to global assessments of phytoplankton dynamics from the SeaWiFS mission. Remote Sens. Environ. 135, 77–91.
Siegel, D., Maritorena, S., Nelson, N.B., Behrenfeld, M.J., 2005. Independence and interdependencies among global ocean color properties: reassessing the bio-optical assumption. J. Geophys. Res. – Oceans 110, C07011. http://dx.doi.org/10.1029/2004JC002527.
Sinclair, M., Keighan, E., Jones, J., 1979. ATP as a measure of living phytoplankton carbon in estuaries. J. Fish. Res. Board Can. 36, 180–186.
Sherr, E.B., Sherr, B.F., Wheeler, P.A., 2005. Distribution of coccoid cyanobacteria and small eukaryotic phytoplankton in the upwelling ecosystem off the Oregon coast during 2001 and 2002. Deep-Sea Res. II 52, 317–330.
Slade, W.H., et al., 2010. Underway and moored methods for improving accuracy in measurement of spectral particulate absorption and attenuation. J. Atmos. Ocean. Tech., 27. http://dx.doi.org/10.1175/2010JTECHO755.1.
Stockner, J.G., Klut, M.E., Cochlan, W.P., 1990. Leaky filters: a warning to aquatic ecologists. Can. J. Fish. Aquat. Sci. 47, 16–23.
Stramski, D., Kiefer, D.A., 1991. Light scattering by microorganisms in the open ocean. Prog. Oceanogr. 28, 343–383.
Strathmann, R.R., 1967. Estimating the organic carbon content of phytoplankton from cell volume or plasma volume. Limnol. Oceanogr. 12, 411–418.
Strickland, J.D.H., 1960. Measuring the production of marine phytoplankton. Bull. Fish. Res. Board Can. 122, 1–127.
Sutherland, G.K., 1913. Some methods of plankton investigation. J. Ecol. 1, 166–176.
Taguchi, S., Laws, E.A., 1988. On the microparticles which pass through glass fiber filter type GF/F in coastal and open waters. J. Plankton Res. 10, 999–1008.
Van Heukelem, L., Thomas, C.S., 2001. Computer-assisted high-performance liquid chromatography method development with applications to the isolation and analysis of phytoplankton pigments. J. Chromatogr. A 910, 31–49.
Veldhuis, M.J.W., Kraay, G.W., 2004. Phytoplankton in the subtropical Atlantic Ocean: towards a better assessment of biomass and composition. Deep-Sea Res. I 51, 507–530.

Verity, P.G., Robertson, C.Y, Tronzo, C.R., Andrews, M.G., Nelson, J.R., Sieracki, M.E., 1992. Relationships between cell volume and the carbon and nitrogen content of marine photosynthetic nanoplankton. Limnol. Oceanogr. 37, 1434–1446.

Vaillancourt, R.D., Brown, C.W., Guillard, R.R.L., Balch, W.M., 2004. Light backscattering properties of marine phytoplankton: relationships to cell size, chemical composition and taxonomy. J. Plankton Res. 26, 191–212.

Wallhead, P.J., Garçon, V.C., Casey, J.R., Lomas, M.W., 2014. Long-term variability of phytoplankton carbon biomass in the Sargasso Sea. Glob. Biogeochem. Cycles 28, 825–841.

Westberry, T.K., Behrenfeld, M.J., Siegel, D.A., Boss, E., 2008. Carbon-based primary productivity modeling with vertically resolved photoacclimation. Glob. Biogeochem. Cycles 22, GB2024. http://dx.doi.org/10.1029/2007GB003078.